

LABORATORY EXPERIMENTS WITH AQUEOUS SOLUTIONS MODELLING MAGMA CHAMBER  
PROCESSES II. COOLING AND CRYSTALLIZATION ALONG INCLINED PLANES

Herbert E. Hupper<sup>1</sup>, R. Stephen J. Sparks<sup>2</sup>, J. Richard Wilson<sup>3</sup>,  
Mark A. Hallworth<sup>1</sup> and Alison M. Leitch<sup>4</sup>

1. Department of Applied Mathematics and Theoretical  
Physics, University of Cambridge, Silver Street, Cambridge CB3  
9EW, England; 2. Department of Earth Sciences, University of  
Cambridge, Cambridge CB2 3EQ, England; 3. Department of  
Geology, Aarhus University, Aarhus, Denmark; 4. Research  
School of Earth Sciences, Australian National University,  
Canberra, Australia

ABSTRACT

Experiments have been carried out on the cooling and crystallization of aqueous solutions of  $\text{Na}_2\text{CO}_3$  along an inclined plane. Compositional stratification is generated in homogeneous solutions both below an overhanging roof and above an inclined floor. Experiments with a ternary system ( $\text{FeSO}_4 - \text{Na}_2\text{SO}_4 - \text{H}_2\text{O}$ ) along a  $45^\circ$  slope showed the same general behaviour. In addition, layering was produced in the solid. Experiments with initially stratified solutions of  $\text{Na}_2\text{CO}_3$  showed that the density gradient suppressed vertical mixing as light fluid was released. The stratified solutions developed thermally driven double-diffusive layers and caused a cusped structure to develop in the crystallization front. Contours of constant  $\text{Na}_2\text{CO}_3$  content in the solid product were discordant to the positions of the crystallization front. In experiments involving large volumes for which the fluid at any height remains essentially constant in composition, the  $\text{Na}_2\text{CO}_3$  content of the solid increased outwards away from the plane. In experiments involving smaller volumes of fluid, slow cooling rates or more complete crystallization of the solution, the  $\text{Na}_2\text{CO}_3$  content of the solid decreased outwards in later stages causing a reversal. One experiment involved replenishment of the tank by an 8 cm layer of concentrated  $\text{Na}_2\text{CO}_3$  solution emplaced at the base of the container. The resident stratified solution was passively lifted and caused the solid to temporarily melt back for a few hours before crystallization recommenced. The replenishment caused the  $\text{Na}_2\text{CO}_3$  content of the solid to increase on the below slope side at all levels.

Marked discordances between rhythmic, phase and cryptic layering have been recorded in layered intrusions. These features have been interpreted in terms of crystallization along inclined margins from compositionally stratified magma (Wilson and Larsen, 1985) and by a lateral accretion model (Irvine et al., 1983) in which rock layers form

from adjacent double-diffusive magma layers. The experiments confirm several features of the lateral accretion model: cusps occur adjacent to double-diffusive layers, compositional contours in the solid do eventually dip inwards to the centre of the tank and light residual liquid tends to move as a boundary layer flow parallel to the margin even along an inclined floor. However, the sense of circulation in the adjacent double-diffusive layers was driven by thermal rather than compositional effects and we failed to produce any solid layering adjacent to and equivalent to the double-diffusive layers. Compositional reversals were generated by replenishment. In the initial stages of experiments decreasing the cooling rate caused an increase in  $\text{Na}_2\text{CO}_3$  content away from the slope and this may be one cause of the basal reversals in cryptic layering observed at the margins of many layered intrusions.

## 1. INTRODUCTION

Crystallization along the margins of a magma chamber often takes place along sloping boundaries. Many layered intrusions show a synformal structure in cross-section with the layering dipping into the interior, indicating that solidification commonly occurs on an inclined floor. The walls of many layered intrusions can also depart from vertical and both inwardly and outwardly inclined walls are known. Experimental studies using aqueous systems to model magma chambers, however, have largely been concerned with crystallization along vertical and horizontal boundaries (Chen and Turner, 1980; McBirney, 1980; Turner and Gustafson, 1981; McBirney et al., 1985; Huppert and Worster, 1985). Irvine's (1981) model for the Muskox intrusion, however, involves crystallization of compositionally stratified magma along a sloping floor. This paper examines the effects of such inclined boundaries.

The angular relationships between different kinds of layering are proving to be of considerable interest. In his concept for crystallization of the Muskox intrusion, Irvine (1981) considered evolution of the large-scale macrocyclic rock units since small-scale modal layering is seldom developed in this intrusion, and he did not consider cryptic variations. However, Wilson and Larsen (1985) have demonstrated that large angular discordances can exist between modal layering and both phase and cryptic layering. This observation has led to the question of how the various kinds of layering and their orientations relate to the solidifying boundaries of magma chambers. Wilson and Larsen (1985) envisaged modal layering as developing parallel to the crystallization front while the discordance to phase and cryptic layering reflects crystallization from a compositionally zoned magma along an inclined boundary. This study considers how fluid dynamical processes along inclined crystallization fronts relate to compositional variations and layering in the resulting solid products.

Section 2 describes the experimental methods and summarises results on crystallization of homogeneous solutions along inclined boundaries which have been reported in detail elsewhere (Huppert et al., 1986) and

describes an exploratory experiment with a ternary system. Section 3 investigates the behaviour of initially stratified solutions of  $\text{Na}_2\text{CO}_3$ . Section 4 reports preliminary measurements on the compositional variations in the solid products and documents how discordances can develop between isocompositional contours and the positions of the crystallization front. Section 5 considers the effects of replenishment on these systems and its influence on the compositional variations in the solid. Section 6 considers the geological applications of the experimental work.

## 2. HOMOGENEOUS SOLUTIONS

### 2.1 Methods

Experiments were conducted in a Perspex container 30 cm high and 7.5 cm wide and whose length could be varied up to 91 cm (Figure 1). The walls, roof and floor of the tank were insulated with polystyrene. The insulation could be removed for observation, which was accomplished using the shadowgraph technique. Coolant was circulated through a thin (1 cm thick) rectangular box made of copper covered with wire gauze. The cooling box could be moved to vary the angle of slope. The experimental system allowed two experiments to be carried out at the same time, with cooling occurring below the slope (an overhanging roof) and above the slope (an inclined floor).

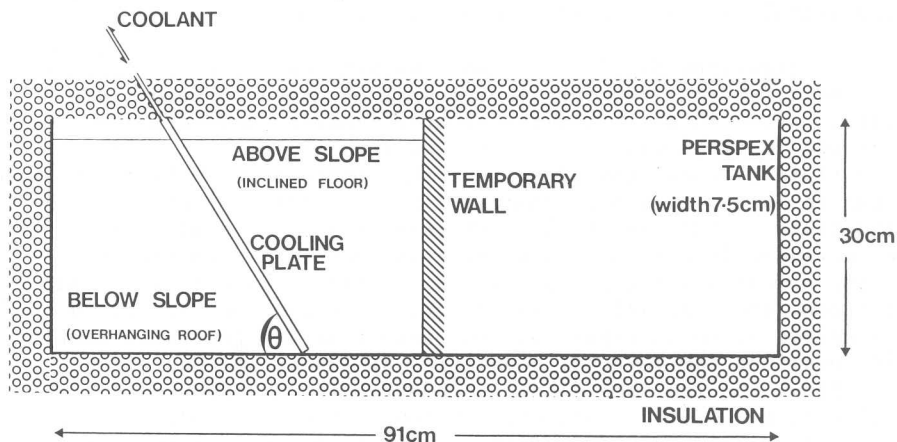


Figure 1. Geometry of apparatus used in experimental studies of cooling and crystallization.

Most of the experiments were carried out using aqueous  $\text{Na}_2\text{CO}_3$  solutions. This system shows simple binary phase equilibria (eutectic at 6.1 wt %  $\text{Na}_2\text{CO}_3$  and  $-2^\circ\text{C}$ ). Details of density and phase relations

have been reported elsewhere (Chen and Turner, 1980; Huppert et al., 1986). The system does not involve nucleation difficulties and compositions can be determined from refractive index measurements. Samples of the solutions were taken by withdrawing a fraction of a cc with a syringe. The solid blocks of ice and salt that formed adjacent to the cooling slopes were sampled by drilling cores (about 1 cm diameter) and cutting several core slices. The refractive index of each sample after dissolving in a known quantity of water. Figure 2 shows the geometries and conditions of the eleven new experiments reported in this paper.

We also report some results of a different experimental technique developed by one of us (A.M. Leitch, 1985) at the Australian National University. In these experiments a tank measuring 20 cm x 16 cm x 15 cm was used in which two of the walls, the roof and the base were built to act as heat exchangers. This apparatus was well insulated and could be sufficiently cooled that the whole contents of the tank could solidify. Experiments where complete freezing of  $\text{Na}_2\text{CO}_3$  solutions were accomplished are described in section 4.

## 2.2 Results with $\text{Na}_2\text{CO}_3$

We first summarise the experimental results reported in Huppert et al. (1986). An experiment involving cooling and crystallization of a 12.8 wt %  $\text{Na}_2\text{CO}_3$  solution along a  $45^\circ$  slope illustrates the major features. We then describe an experiment with a more complicated chemical system ( $\text{Na}_2\text{SO}_4 - \text{FeSO}_4 - \text{H}_2\text{O}$ ), which illustrates the sensitivity of the observed effects to the composition of the system.

**2.2.1 Homogeneous  $\text{Na}_2\text{CO}_3$  solution.** Within the first few minutes of an experiment, thermal boundary layers were observed on both sides of the plate. After 10 to 15 minutes crystallization commenced along both sides of the inclined plane. On the overhanging wall, buoyant released fluid ascended the slope in a thin compositional boundary layer and began to form a region of compositionally stratified and solute-depleted fluid at the top of the tank (Figure 3a). The stratified region increased in thickness with time and was separated from an underlying homogenous region by a sharp interface (Figure 3a). Four compositional profiles and a phase diagram illustrating the initial conditions are shown in Figure 4. The behaviour was generally similar to that described for vertical boundaries by Turner and Gustafson (1981). Above the inclined floor the buoyant fluid released from the crystallizing  $\text{Na}_2\text{CO}_3 \cdot 10\text{H}_2\text{O}$  ascended in numerous thin plumes ( $< 1$  mm wide) as seen in Figure 3(a and b). Stratification also developed (Figure 4a) but was noticeably weaker than that on the overhanging roof side. A steep gradient appeared at the top and graded down to the weakly stratified solution in the central and lower region. Compositional stratification then developed throughout the solution on both sides with prominent double-diffusive layers (Figures 3b and 3c). Eventually an homogeneous layer of eutectic composition formed at the top which gradually extended through most of the solution (Figure 4).



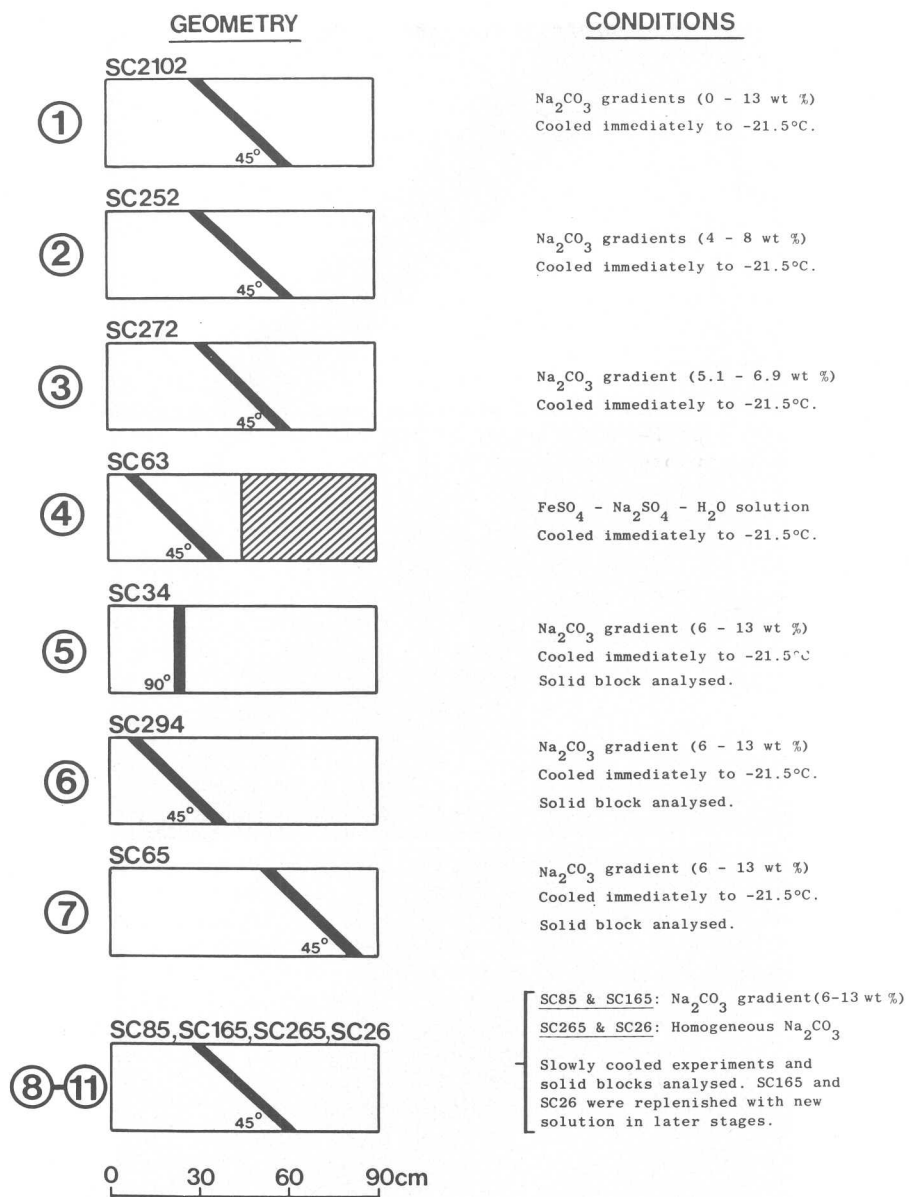


Figure 2. Illustration of the geometry and conditions of the eleven experiments reported in this paper.

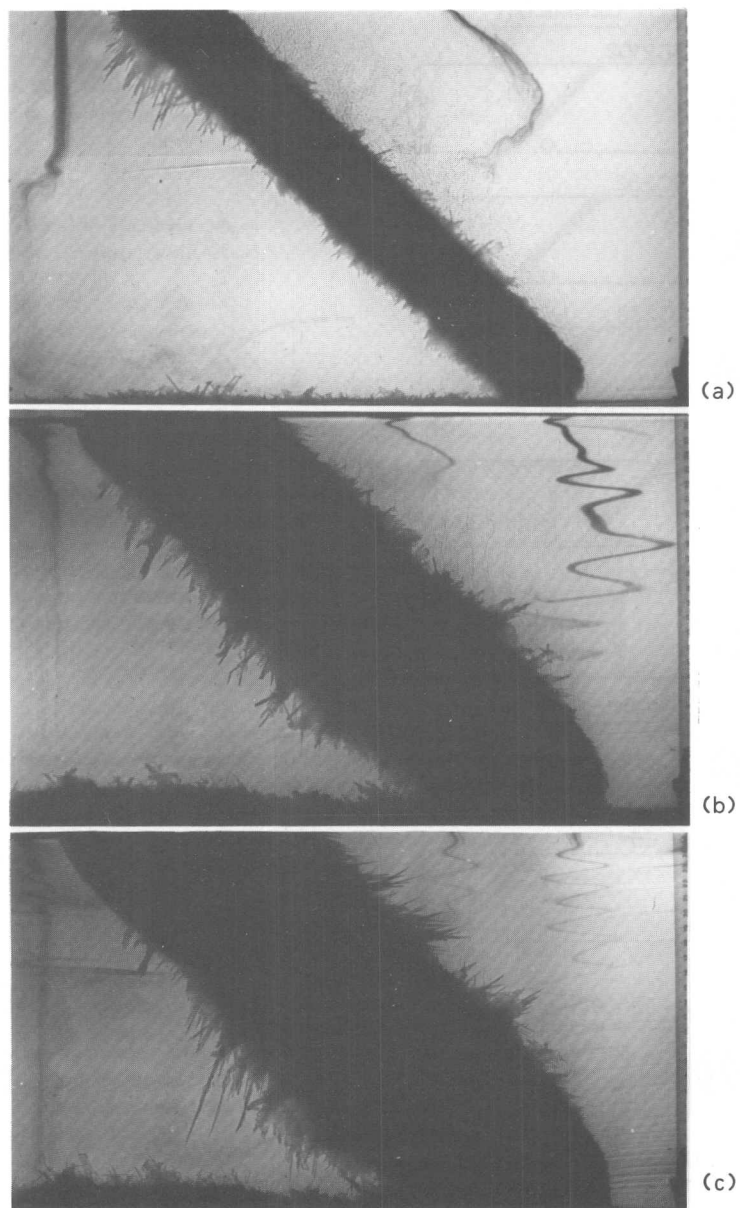


Figure 3. Three photographs of an experiment in which a homogeneous solution of  $\text{Na}_2\text{CO}_3$  was cooled along a  $45^\circ$  inclined plane: (a) 80 mins; (b) 5 hr, and (c) 8 hr, after the commencement of the experiment. In each case, a vertical line of  $\text{KMnO}_3$  dye was added a moment before the photographs were taken.

Experiments are also described by Huppert et al. (1986) with different slope angles and different ratios of width to depth. Experiments with angles of  $90^\circ$ ,  $70^\circ$  and  $20^\circ$  showed the same broad behaviour. Even with the floor inclined at only  $20^\circ$  compositional stratification still developed. Stronger compositional gradients developed in tanks with larger ratios of width to depth.

An important result of these experiments is that a strong compositional boundary layer flow develops along inclined floors. Although the motion appears to involve vertically-moving, thin plumes, injection of dye at the base of the slope demonstrated that a major part of the motion is up the slope rather than vertical (see Figure 3a). This results in differentiated fluid reaching the top with limited mixing and explains the development of compositional gradients in the liquid. The experiments show that compositional zoning can occur by crystallization along an inclined floor even if the angle is quite small.

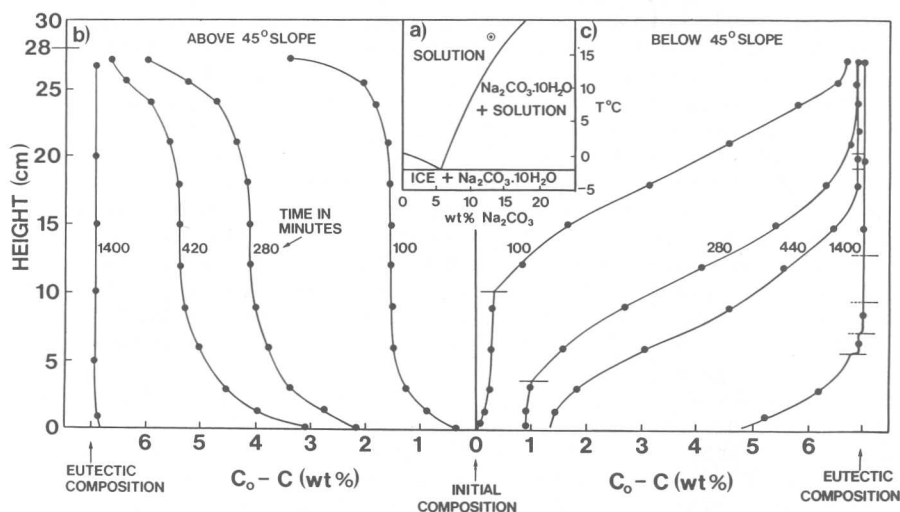


Figure 4. Compositional profiles of  $\text{Na}_2\text{CO}_3$  in an experiment in which an initially homogeneous solution of  $\text{Na}_2\text{CO}_3$  was cooled along a  $45^\circ$  inclined plane. Times of each profile are in minutes. The inset shows the  $\text{Na}_2\text{CO}_3 - \text{H}_2\text{O}$  phase diagram, and represents the starting conditions.

An important aspect of the experiments was the physical structure in the crystallizing front. In most experiments the coolant temperature was reduced to  $-21.5^\circ\text{C}$ , well below the eutectic ( $-2^\circ\text{C}$ ) of the  $\text{Na}_2\text{CO}_3 - \text{H}_2\text{O}$  system. Solution trapped between  $\text{Na}_2\text{CO}_3 \cdot 10\text{H}_2\text{O}$  dendrites was gradually converted to an ice- $\text{Na}_2\text{CO}_3 \cdot 10\text{H}_2\text{O}$  mix. Thus for non-eutectic compositions the crystallization front consisted of a 'mushy' zone of  $\text{Na}_2\text{CO}_3 \cdot 10\text{H}_2\text{O}$  dendrites growing away from the slope followed by a sharp eutectic front containing ice. The material was totally solid behind

the eutectic front. The mushy zone varied from several cm thick for compositions richer in  $\text{Na}_2\text{CO}_3$  than the eutectic to negligible for eutectic compositions, for which the front was a sharp solid-liquid interface. The crystals in the mushy zone formed a very irregular and poorly defined boundary in experiments below the slope, whereas the mushy zone was much more compact on the side above the slope and formed a well-defined smooth boundary marked by the tips of the dendrites (Figure 3a).

### 2.3 $\text{FeSO}_4 - \text{Na}_2\text{SO}_4 - \text{H}_2\text{O}$

In this exploratory experiment (number 4 of Figure 2) a homogeneous solution of 19.4 wt %  $\text{FeSO}_4$  and 8.3 wt %  $\text{Na}_2\text{SO}_4$  was prepared at  $30^\circ\text{C}$  and then left overnight to come to room temperature ( $15.9^\circ\text{C}$ ). The solution became saturated and small (1 mm) equant crystals of  $\text{FeSO}_4 \cdot 7\text{H}_2\text{O}$  formed and settled to the floor of the container. On starting the cooler, compositional convection began almost immediately on the  $45^\circ$  slope and competed with strong downward thermal motions similar to those observed in the  $\text{Na}_2\text{CO}_3$  experiments. Below the slope many minute crystals rained down from the inclined plane where they had nucleated but failed to attach. By 45 minutes thin white dendrites of  $\text{Na}_2\text{SO}_4 \cdot 10\text{H}_2\text{O}$  had successfully nucleated on both sides of the plane, whereas  $\text{FeSO}_4 \cdot 7\text{H}_2\text{O}$  crystals were still settling out. The solution was clearly saturated in both phases, yet quite efficient separation occurred on the side below the slope because of kinetic and morphological factors operating at the main cooling surface. A layer entirely composed of  $\text{FeSO}_4 \cdot 7\text{H}_2\text{O}$  had formed on the floor of the tank where continued growth was evident by compositional convection. The layer forming beneath the inclined roof was enriched in  $\text{Na}_2\text{SO}_4 \cdot 10\text{H}_2\text{O}$ . Above the slope many of the small equant  $\text{FeSO}_4 \cdot 7\text{H}_2\text{O}$  crystals had settled onto the inclined plane to form a discrete layer (Figure 5).

From the fluid dynamical viewpoint, the main features of the experiment were the same as the  $\text{Na}_2\text{CO}_3$  system. Thin plumes ascended from the crystallization front above the slope and the development of a weak density gradient was apparent. Below the slope, as before, a strong gradient region developed with a sharp interface separating it from a more homogeneous region below. Compositional convection from the settled  $\text{FeSO}_4 \cdot 7\text{H}_2\text{O}$  layer helped to maintain the homogeneity of the lower region. After a few hours double-diffusive layering developed on both sides.

By 3 hours yellow-green dendritic crystals of  $\text{FeSO}_4 \cdot 7\text{H}_2\text{O}$  were also observed to be forming amongst the  $\text{Na}_2\text{SO}_4 \cdot 10\text{H}_2\text{O}$  dendrites in the crystallized layers growing adjacent to the plane. A sharp front which grew about 1 cm behind the dendritic front was interpreted as the position of the eutectic front containing ice. The dendritic  $\text{FeSO}_4 \cdot 7\text{H}_2\text{O}$  crystals were much coarser than the  $\text{Na}_2\text{SO}_4$  crystals and each dendrite branch was observed to be composed of many stubby crystals in a chain or array, giving dendrites a rough sturdy appearance. By 8 hours the solid layer below the slope had grown to 3.5 cm thick. The upper 16 to 27 cm region of the solid layer was noticeably poor in  $\text{FeSO}_4 \cdot 7\text{H}_2\text{O}$  crystals and was surmised to be largely  $\text{Na}_2\text{SO}_4 \cdot 10\text{H}_2\text{O}$  and ice growing from the upper

gradient region which had been strongly depleted in  $\text{FeSO}_4 \cdot 7\text{H}_2\text{O}$ . A gradational boundary between  $\text{FeSO}_4 \cdot 7\text{H}_2\text{O}$ -rich and -poor solid was visible and was vertical at about 16 cm height, discordant to the solidification front. A sketch of the layering after 23 hours is shown in Figure 5. Towards the later stages of the experiment as the cooling rate diminished large rhombohedral crystals up to 1 cm in diameter had formed on all the walls and floor of the perspex tank forming a compact layer above the layer of much finer crystals (Figure 5). Three quite different sizes and shapes of  $\text{FeSO}_4 \cdot 7\text{H}_2\text{O}$  had formed during the experiment depending on their environment of nucleation and growth.

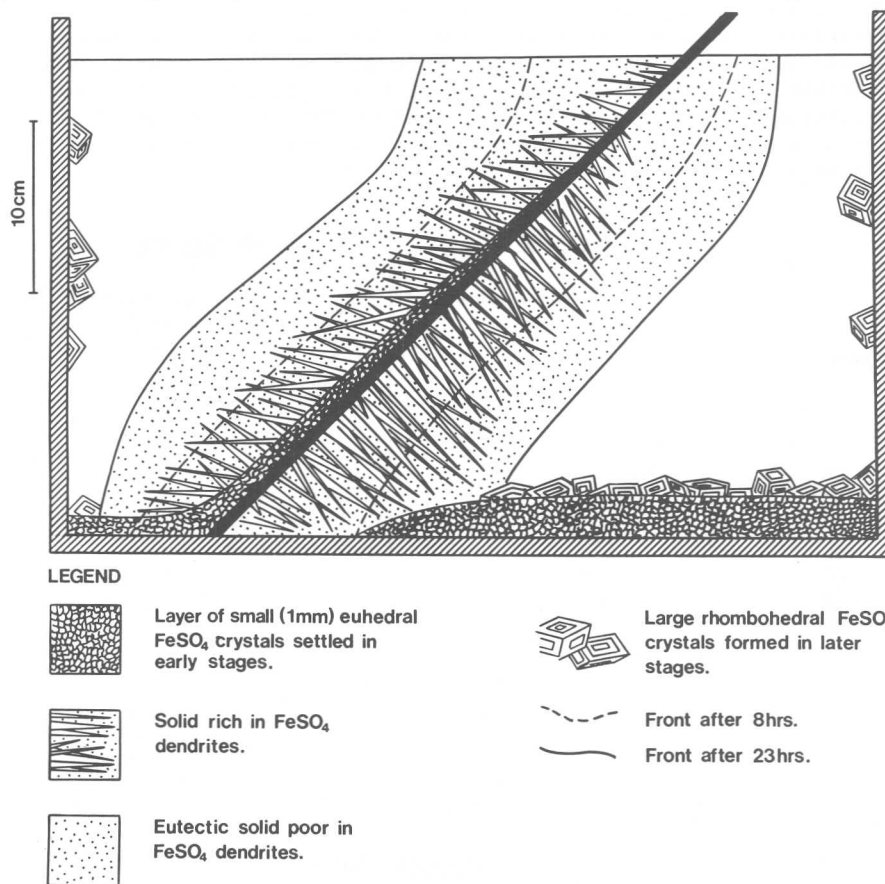


Figure 5. Schematic diagram showing distribution of different textural varieties of  $\text{FeSO}_4 \cdot 7\text{H}_2\text{O}$  and  $\text{NaSO}_4 \cdot 10\text{H}_2\text{O}$  in experiment 4.

The experiment nicely demonstrates the sensitivity of crystal morphology and size to kinetic effects and to the nature of the particular chemical system. It also illustrates that crystals can nucleate and grow in places that are a long way from the boundary where

heat is being lost. Crystals can nucleate and grow in distant sites, because of the convection which allows heat loss from one boundary to be manifested by crystallization at other insulated boundaries. The experiment also produced discordant layering, which is more fully considered in the next sections.

### 3. EFFECTS OF STRATIFICATION

In all the experiments reported by Huppert et al. (1986), initially homogeneous solutions became stratified as a consequence of the crystallization along the inclined plane. We now report a series of experiments with solutions which were initially stratified so that we could observe how the compositional convection interacts with the stratification. We will first describe experiment 2 of Figure 2 in detail and then consider variations in initial gradient, slope and tank geometry in the other experiments.

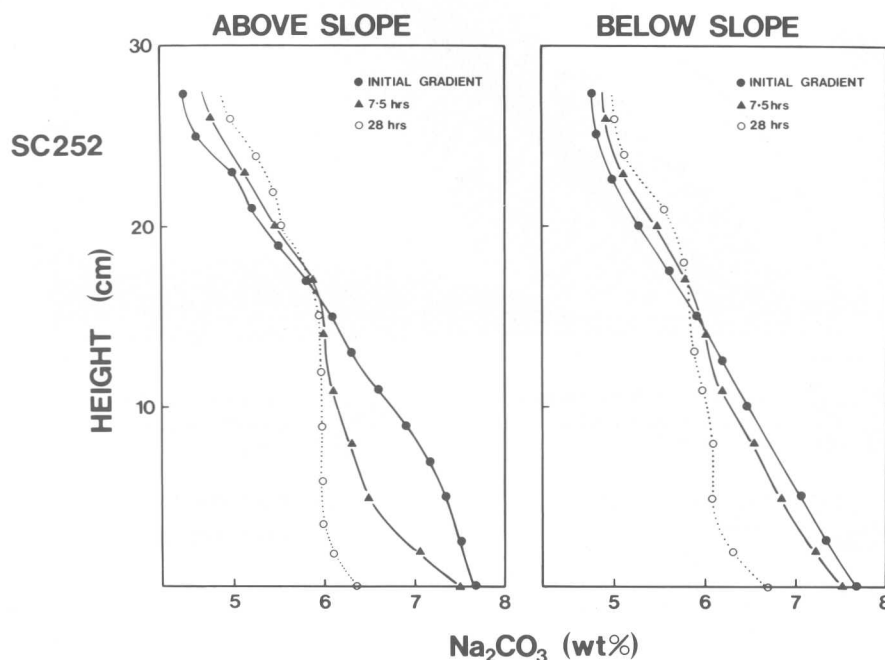


Figure 6. Compositional profiles at various times in experiment (2).

Experiment (2) involved an initially linear gradient of  $\text{Na}_2\text{CO}_3$  solution with a concentration of 4.5 wt % at the top and 7.7 wt % at the bottom (Figure 6). An interesting feature of this gradient is that the eutectic composition (6.0 wt %  $\text{Na}_2\text{CO}_3$ ) occurs at about 16 cm height and

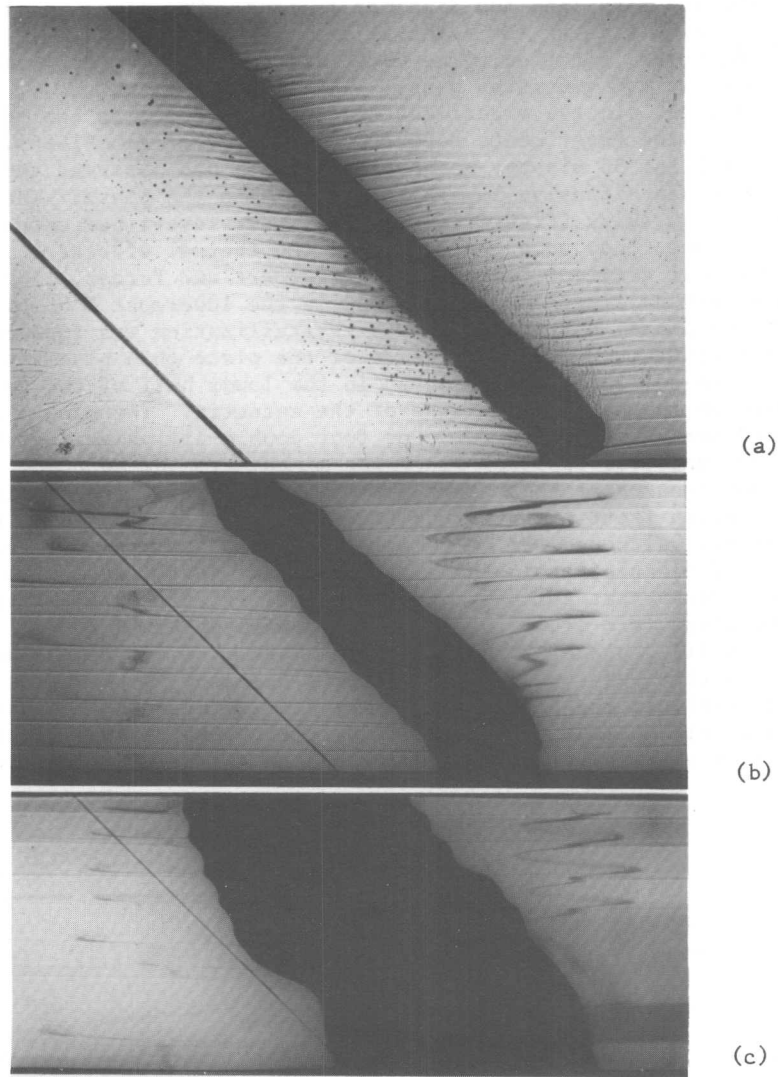


Figure 7. Photographs of experiment (2) in which cooling and crystallization of a stratified solution of  $\text{Na}_2\text{CO}_3$  occurs along an inclined plane. Well-developed double-diffusive layers can be seen. (a) After 23 minutes thermally driven double-diffusive layers intruded laterally into stratified solution; (b) After 2 hours significant solidification occurred, producing a cusped crystallization front with each cusp being associated with a double-diffusive layer. Dye streak shows sense of motion in layers. (c) After 24 hours solidification front shows large cusps and double-diffusive layers. The thin slanted line 12 cm to the left of the cooling box is a milled groove in the wall of the perspex tank.

divides the solution into two distinct regions. The lower region is on the  $\text{Na}_2\text{CO}_3$ -rich side of the eutectic and generates light residual solution on crystallization. The upper region is on the ice-rich side of the eutectic and generates dense residual solution on crystallization. In the experiment the cooler was set to cool down to  $-21.5^\circ\text{C}$  as in the experiments reported by Huppert et al. (1986).

In the first 30 minutes no crystallization was observed and a series of double-diffusive layers formed next to the plate. The layers were about 1 cm thick (Figure 7a) and by 1 hour layers had extended across the tank. They were formed due to the thermal effects of cooling a compositional gradient from the side (Huppert and Turner, 1980). By 45 minutes crystallization was observed in the lowermost 5 cm of both sides of the plate, and by 90 minutes crystallization was apparent along its entire length. On the upper side of the plate thin plumes of buoyant released fluid were observed in the lower half of the tank in the region on the  $\text{Na}_2\text{CO}_3$ -rich side of the eutectic. The plumes rarely penetrated across more than three or four double-diffusive interfaces (Figure 7a) and most residual fluid was mixed into the adjacent layer. A prominent feature at this stage was the development of cusps in the crystallization front (Figure 7b,c and 8) which corresponded to adjacent fluid layers. Although the compositional convection was quite vigorous, the sense of circulation in the interior of the double-diffusive layers was in the sense that corresponded to thermal effects at all levels. Below the slope thin plumes of dense fluid were observed to fall away from the inclined plane at heights above 20 cm, whereas plumes were only observed to rise away on the above slope side below 20 cm height. This behaviour reflects the difference in the density effects of crystallization on either side of the eutectic, with dense residual fluid on the ice-rich side and light residual fluid on the  $\text{Na}_2\text{CO}_3$ -rich side.

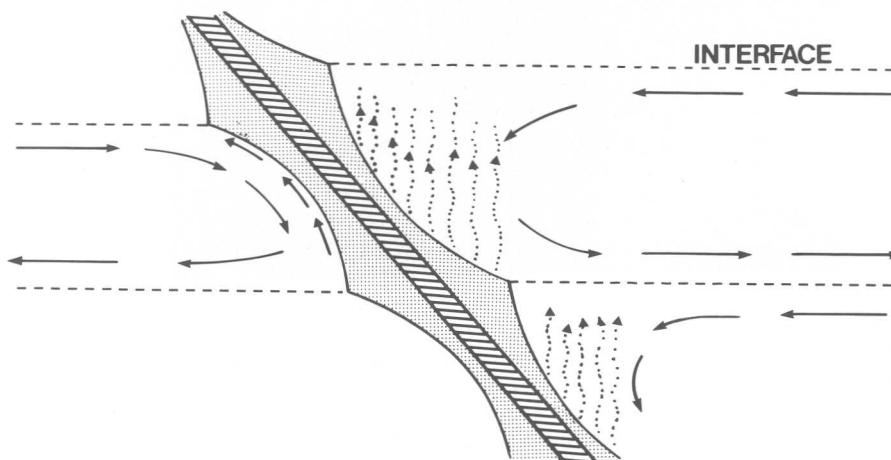


Figure 8. Schematic diagram showing circulation patterns in double-diffusive layers adjacent to the crystallization front during cooling and crystallization of a  $\text{Na}_2\text{CO}_3$  gradient.



The physical appearance and behaviour of the two sides continued in much the same way up to 13 hours when the tank was left unobserved overnight. Compositional profiles taken at 7.5 hrs (Figure 6) show that the evolution of the two sides involved a gradual weakening of the gradients as the fluid at all levels evolved towards the eutectic composition. Similar behaviour was observed in the later stages of experiments with initially homogeneous solutions (Huppert et al., 1986).

After 23 hours both sides had developed into two distinct regions (Figure 7c). Below 17 cm there was weak compositional convection on the above slope side and the fluid was very weakly layered on both sides. The solidification fronts were quite smooth and no cusps were present. The composition of the fluid had reached the eutectic at most levels below 17 cm (Figure 6). Above 17 cm four well-developed double-diffusive layers had developed on both sides and the solidification front had developed strong cusps corresponding to the layers. There was still a marked compositional gradient in this region (Figure 6).

Two other experiments (1 and 3) were performed with the same geometry, but different gradients (Figure 2). The spacing of the double-diffusive layering decreased with a stronger gradient (experiment 1) to a few millimetres and increased with the weaker gradient (experiment 3) to between 2 and 3 cm. This is in accordance with theoretical predictions (Huppert and Turner, 1980). In other respects the behaviour of the experiments was similar. In experiment 3 the cusps and their associated double-diffusive layers were observed to progressively migrate upwards with time on the above slope side at heights above 13 cm. No layering corresponding to adjacent double-diffusive layers was observed in the solid. No consistent pattern of cusp or layer migration was observed on the below slope side.

Experiments with a vertical boundary (5) and with different volumes (experiments 6 to 9) showed the same behaviour. Common features observed in all runs include the following:

- (i) The density gradients had a strong restraining influence on the compositional convection with thin plumes only occasionally moving through the interfaces of overlying double-diffusive layers.
- (ii) The circulation in double-diffusive layers was controlled by thermal effects even in regions where composition convection might potentially oppose the motion.
- (iii) The gradients always weakened with time as the fluid systems evolved towards the eutectic.
- (iv) Cusps sometimes developed adjacent to double-diffusive layers (Figure 7 and 8). They were better developed when the composition of fluid was on the ice-rich side of the eutectic where dense residual fluid is generated. The cusps were less prominent or were not observed on the  $\text{Na}_2\text{CO}_3$  side of the eutectic where light residual fluid is released.

#### 4. COMPOSITIONAL VARIATIONS IN THE SOLIDS

Much of the research using aqueous solutions has emphasised the fluid dynamical phenomena and the compositional variations that develop in the liquid. In this section we present the results of preliminary experiments on the compositional variations in the solid product. Many questions remain unanswered, but we hope that a description of the work up to this time will stimulate further, more complete, discussion.

##### 4.1 Cooling a $\text{Na}_2\text{CO}_3$ gradient along a vertical wall

In this experiment (number 5) the tank was divided into two unequal parts (Figure 2) with volumes of 4.7 and 14.8 litres respectively. A linear gradient was created from near the eutectic composition of 6.2 wt %  $\text{Na}_2\text{CO}_3$  at the top to 13.0 wt % at the base. The evolution of the compositional gradients on the two sides is presented in Figure 9, which shows that after 24 hours the smaller volume eventually evolved to the eutectic composition at all levels, whereas the larger volume was still compositionally stratified.

During the experiment the fluid dynamical behaviour of the two sides was similar to previously described experiments. The initial fluid broke up into many double-diffusive layers slightly over 1 cm in average thickness. In the smaller volume the layering weakened towards the end of the experiment as the solution approach a uniform eutectic composition. A slightly cusped structure to the crystallization front developed on both sides, but no corresponding structure was preserved in the interior of the solid.

Figure 10 shows contours of equal composition in the solid and an estimate of the position of the crystallization front after 5 hours. The most significant feature of the data is that contours of constant composition in the solid are discordant to the contours representing the position of the crystallization front at different times. Broadly the composition of the solid becomes more water-rich upwards, which reflects the compositional stratification in the adjacent solution.

A significant difference is apparent between the two sides in the inclination of the compositional contours with respect to the vertical wall. In the larger volume the solid becomes more  $\text{Na}_2\text{CO}_3$  rich away from the wall on any given height, whereas the solid decreases in  $\text{Na}_2\text{CO}_3$  away from the wall on the smaller volume side. An important feature of the data is that the solid at any position is always richer in  $\text{Na}_2\text{CO}_3$  than the adjacent fluid from which it formed, except when the fluid had the eutectic composition.

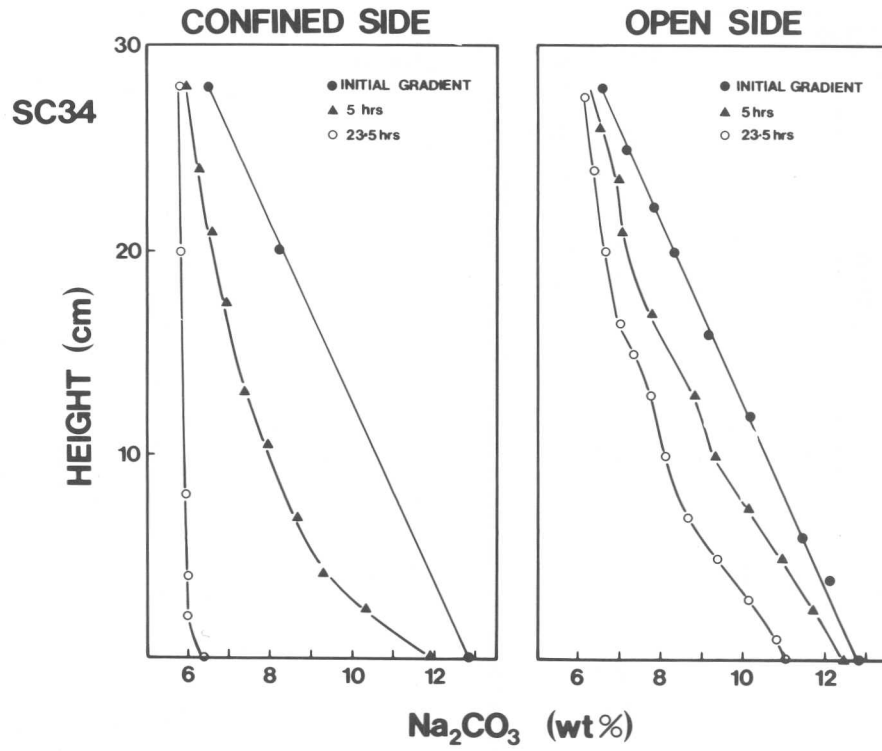


Figure 9. Compositional profiles at various times in experiment (5).

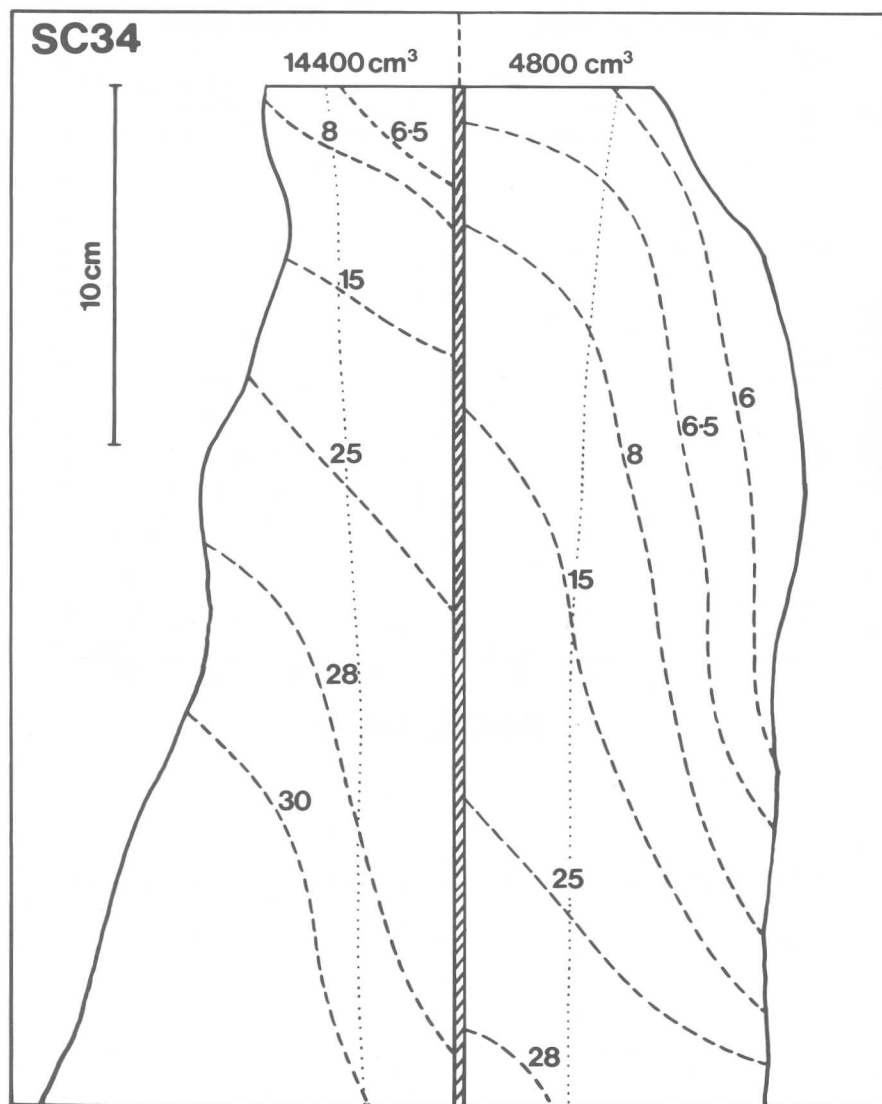


Figure 10. Contours of constant composition in the solid of experiment (5) in weight percentage Na<sub>2</sub>CO<sub>3</sub>. Dotted line shows position of solidification front after 5 hours.

#### 4.2 Cooling a $\text{Na}_2\text{CO}_3$ gradient along a $45^\circ$ slope

Figure 11 shows the results of cooling at an inclined plane of slope  $45^\circ$ . Four experiments were carried out so that results with large and small volumes on both sides of the slope could be compared (Figure 11). The experiments show the same essential features as the vertical wall with discordance between compositional contours and the crystallization front and vertical gradients which reflect the compositional stratification in the fluid. In experiments with the smaller volume of fluid both the inclined floor and overhanging roof cases produced an outward decrease in  $\text{Na}_2\text{CO}_3$ , although there is an indication of  $\text{Na}_2\text{CO}_3$  initially increasing away from the slope towards the base in the case of the overhanging roof (Figure 11). For the larger volume case on the overhanging roof side there is an increase in  $\text{Na}_2\text{CO}_3$  away from the slope as was observed for the vertical wall. However, on the inclined floor there is a clear reversal with the  $\text{Na}_2\text{CO}_3$  content reaching a maximum about half-way through the solid and then declining outwards. A notable feature of the small volume case along an inclined floor (Figure 11) is that the compositional contours are almost parallel to the position of the solidification front with only slight discordances, although a strong compositional gradient existed in the adjacent liquid.

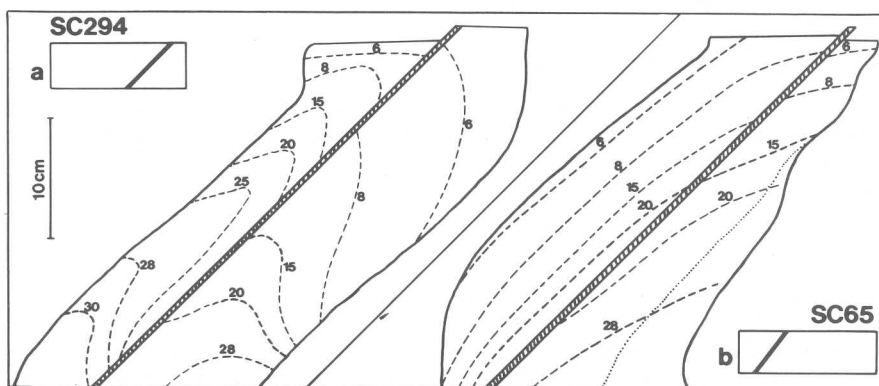


Figure 11. Contours of constant composition in the solid of experiments (6) and (7) in weight percentage  $\text{Na}_2\text{CO}_3$ .

The experiments described above involved rapid cooling of the plate to  $-21.5^\circ\text{C}$ . A slow cooling rate experiment (8) was completed (Figure 12) involving cooling along a  $45^\circ$  slope with the temperature at the plate being decreased in steps of  $5^\circ\text{C}$  over a period of 4 days. The volumes of fluid on the two sides were equal. In this case a decrease in  $\text{Na}_2\text{CO}_3$  content away from the slope occurred on both sides, except near the base.

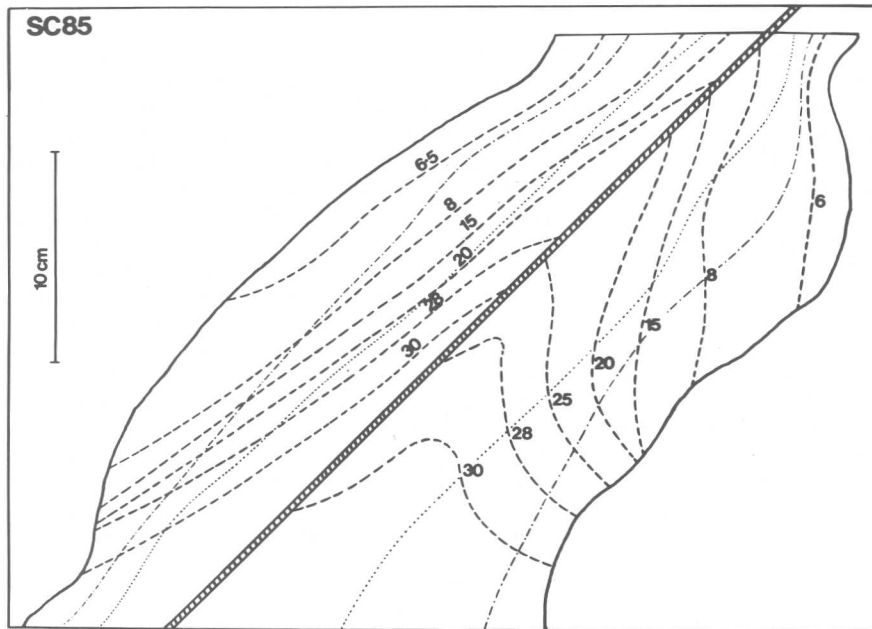


Figure 12. Contours of constant composition in the solid of experiment (8) in weight percentage  $\text{Na}_2\text{CO}_3$ . Solidification fronts at 55 hours (dotted lines) and 73 hours (dash-dot lines) are shown.

#### 4.3 Complete freezing of homogeneous systems

These experiments involved the apparatus at the Australian National University (Leitch, 1985). A glass tank was cooled from one wall, which was rapidly brought to a temperature of  $-18^\circ\text{C}$  at the beginning of the experiment. The solution was completely solidified by 24 hours, so the crystallization rates were considerably faster than in the Cambridge apparatus. The results of an experiment in which the initial homogeneous composition was on the  $\text{Na}_2\text{CO}_3$ -rich side of eutectic (8.8 wt %  $\text{Na}_2\text{CO}_3$ ) will be outlined here.

The experiment with 8.8 wt %  $\text{Na}_2\text{CO}_3$  produced the typical fluid dynamical effects of cooling and crystallization at a vertical boundary with a compositional boundary layer and the development of compositional stratification above a sharp interface which migrated down with time. Eventually all the solution reached the eutectic composition. The crystallization front was approximately vertical throughout the experiment. Until the eutectic composition was reached, the front had

the appearance of a mushy zone of minute  $\text{Na}_2\text{CO}_3$  crystals followed by a eutectic front containing ice.

The compositional variations shown in the experiments (Figure 13) show the same features as the previously described experiments. Horizontally the solid initially becomes richer in  $\text{Na}_2\text{CO}_3$  away from the wall, reaches a maximum and then decreases outwards until the solid has a uniform eutectic composition. Except near the base the  $\text{Na}_2\text{CO}_3$  content decreases with height reflecting the development of compositional gradients during the course of an experiment. Compositional contours are again discordant to the positions of the near vertical crystallization front.

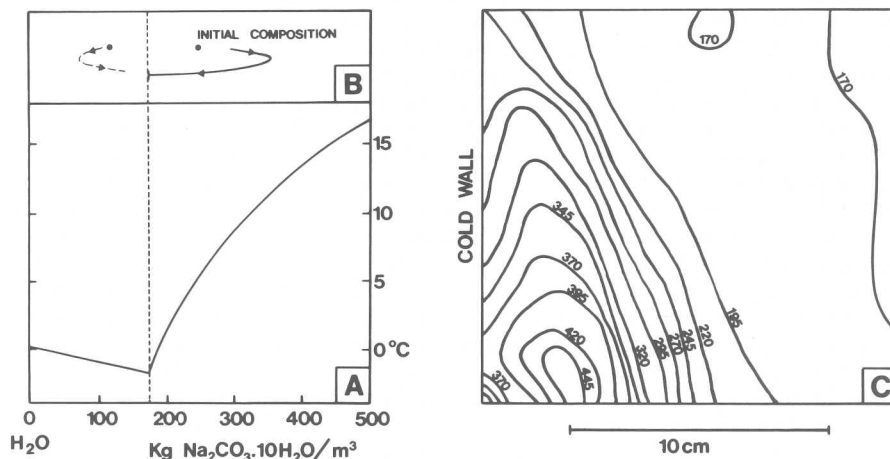


Figure 13. A. Phase diagram of  $\text{Na}_2\text{CO}_3$  system is shown in units of  $\text{Kg}$  of  $\text{Na}_2\text{CO}_3 \cdot 10\text{H}_2\text{O}$  per cubic metre of solution; B. Compositional variation in solution; C. Compositional contours of  $\text{Na}_2\text{CO}_3$  content (in units of  $\text{Kg}$  of  $\text{Na}_2\text{CO}_3 \cdot 10\text{H}_2\text{O}$  per cubic metre of solution) in solid. Dimensions of solid in cross-section are 16 cm high and 15 cm high.

Finally we briefly mention experiments comparable to those outlined above on cooling  $\text{Pb-Sn}$  melts along a vertical wall by Hebditch (1975). Similar discordant relationships between the trace of the advancing crystallization front and the  $\text{Pb}$  and  $\text{Sn}$  concentrations in the solid alloy were produced. These experiments provide additional evidence that the features and behaviour that have been documented are general and occur in fluids of widely different properties.

#### 4.4 Interpretations

Two extreme situations can be identified in solidification from a solution of non-eutectic composition. At one extreme the solid can have an identical composition to the liquid. This circumstance requires that there is no differential fluid motion or that any motion does not

modify the local liquid composition. For non-eutectic compositions the solid will approach the liquid-composition if the cooling rate is very fast and can be likened to the chilled margin of an intrusion. At the other extreme the solid can consist entirely of the phase or phases on the liquidus of the adjacent fluid. In the context of the present experiments the solid would only consist of  $\text{Na}_2\text{CO}_3 \cdot 10\text{H}_2\text{O}$  crystals (equivalent to 37 wt %  $\text{Na}_2\text{CO}_3$ ) and no ice. In the context of layered intrusions such a solid can be termed an adcumulate. Formation of such a solid is favoured by slow cooling and crystallization rates so that the residual liquid has time to convect away. The data in Figures 10 to 13 show that neither extreme was actually achieved in the experiments and that the solids had compositions in between that of the liquid and that of the liquidus phase ( $\text{Na}_2\text{CO}_3 \cdot 10\text{H}_2\text{O}$ ). In geological parlance these solids are analogous to orthocumulates and mesocumulates, depending on the proportion of trapped liquid components.

Two competing effects are thought to control the variation of the solid composition in the experiments. First, cooling rate in all the experiments decreased with time as the width of the solid layer increased. Consequently the solid should be closest to a quenched liquid composition at the beginning of an experiment and should become richer in  $\text{Na}_2\text{CO}_3$  as the cooling rate diminishes. This effect is clearly seen in the experiments with large volumes of solution, where there was limited compositional evolution in adjacent fluid at any given level during the period of the experiment (Figures 9 to 12). The effect is also evident in the complete freezing experiment (Figure 13). Second at any given height the fluid changes composition with time as  $\text{Na}_2\text{CO}_3$  is extracted by crystallization. This has the opposite effect, producing a decrease in  $\text{Na}_2\text{CO}_3$  content away from the wall. This effect is best observed in the smaller volume experiments (Figures 9 and 11) where the solution evolves rapidly and has reached the eutectic in most places during the experiments.

In some experiments (Figures 11 and 13) the influence of decreasing cooling rate is initially important, but is eventually replaced by the influence of compositional evolution of adjacent liquid. This results in a maximum in the horizontal variation of  $\text{Na}_2\text{CO}_3$  content and a reversal in the trend.

In all experiments the discordance between compositional contours and the position of the crystallization front can be attributed to the presence of a pre-existing compositional gradient or to the creation of a gradient in an initially homogeneous solution.

## 5. EFFECTS OF REPLENISHMENT

In this section we describe an experiment (number 10) in which the tank was replenished by new solution part of the way through the experiment. We adopted the same conditions as experiment 6 (see Figure 2) in which a stratified solution (6.1 to 13 wt %  $\text{Na}_2\text{CO}_3$ ) was cooled slowly over a period of 4 days along a  $45^\circ$  inclined plane. After 73 hours when the coolant had reached  $-15^\circ\text{C}$  the top 10 cm of solution was drained off each side and a dense layer of 13 wt %  $\text{Na}_2\text{CO}_3$  solution at  $16.7^\circ\text{C}$  was emplaced



along the base of the tank. The new layer was dyed green so that any redistribution of residual fluid within the tank could be observed. The effects of replenishment were observed for two hours and then the coolant temperature was decreased to  $-21.5^{\circ}\text{C}$  and left overnight so that further solidification could take place.

The course of the experiment up to the replenishment followed closely the course observed in all other experiments. Figure 14 shows the initial and final compositional gradients after 72 hours on the two sides of the inclined plane. Between 72 and 73 hours the coolant temperature was decreased from  $-10^{\circ}\text{C}$  to  $-15^{\circ}\text{C}$  just before replenishment at 73 hours. Compositional profiles are shown just after replenishment in Figure 14. The replenishment on the overhanging roof side was initially too fast and some mixing occurred to produce a steep gradient region between 6 and 8 cm. On the inclined floor side the replenishment was much smoother with little mixing and a very sharp interface formed at 8 cm. The compositional gradients above the replenished volume was consistent with passive uplift by 8 cm of the pre-existing solutions. These solutions had reached a near eutectic composition except for the basal 10 cms or so which still had a noticeable gradient.

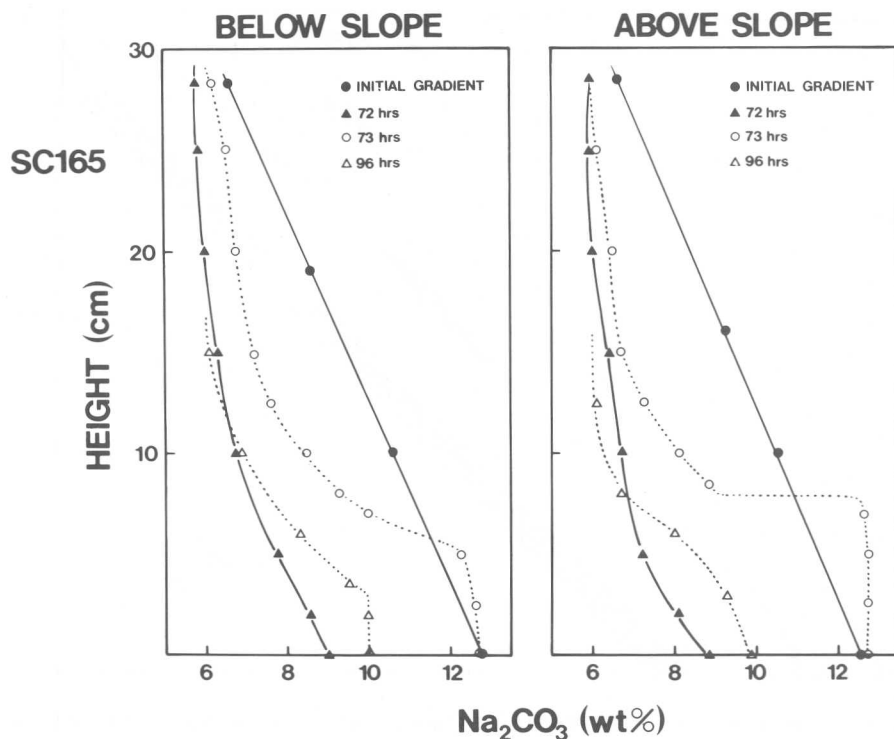


Figure 14. Compositional gradients in experiment (10) with gradients before (solid symbols) and after (open circles) replenishment.

About 40 minutes after replenishment it became clear that some remelting of the solid layer had occurred. This was most apparent along the inclined floor between 10 cm and 20 cm height where the front melted back up to 0.6 cm (Figure 15). Replenishment has in this region replaced eutectic solution by warmer non-eutectic fluid from the uplifted basal gradient fluid. Above 20 cm the fluid remained at the eutectic composition after replenishment which accounts for the absence of remelting. Adjacent to the replenished layer compositional convection was soon apparent and no melting back was apparent. These observations indicate that crystallization had initiated quickly. On the overhanging roof side the crystallization front remained static for the first hour above 13 cm height. After an hour residual fluid from the replenished layer was observed intruding into the double-diffusive layers in the gradient region at 8 to 13.5 cm, above the interface, showing that crystallization had recommenced adjacent to the replenished layer and light residual fluid was rising beneath the roof. At  $4\frac{1}{2}$  hours after replenishment it was clear that crystallization had recommenced at all levels along both sides.

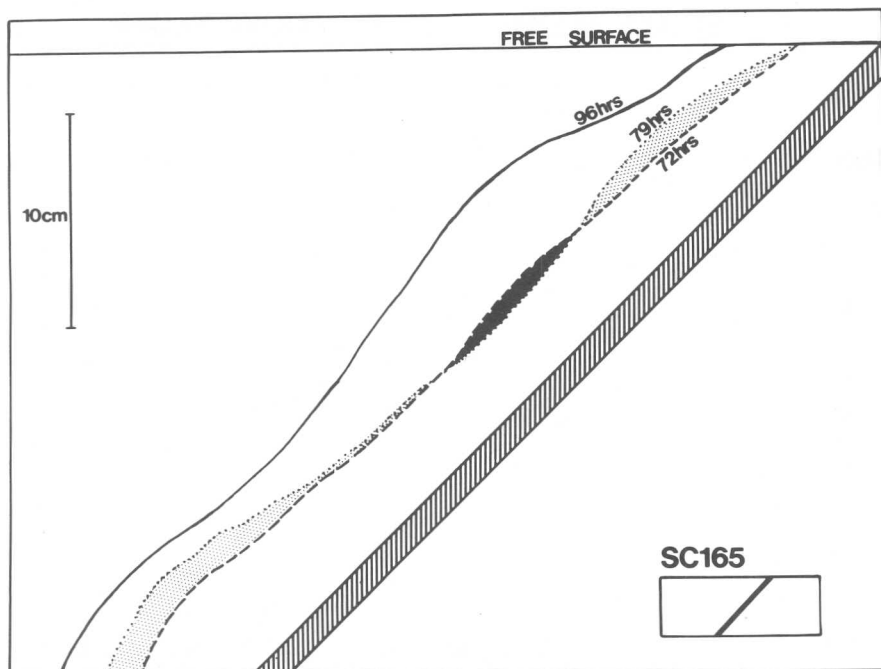


Figure 15. Position of solidification front above the slope just before (72 hrs), 6 hours after replenishment (79 hrs) and 23 hours after replenishment (96 hrs) in experiment (10). Stippled areas showed new growth shortly after replenishment whereas dark central area shows region of melting back.

At 23 hours after replenishment, substantial growth had occurred (Figure 15). On the overhanging roof side the basal replenished layer had decreased to 4 cm thick. Dye had been distributed throughout the upper region and the solid grown since replenishment was dyed at all heights. These observations show that fluid from the replenished layer had been drawn laterally towards the crystallization front where residual fluid ascended up in a boundary layer flow beneath the roof to be distributed throughout the upper layer. Slightly more crystal growth was apparent adjacent to the replenished layer. On the inclined floor side there had been substantial growth adjacent to the replenished layer (Figure 15) forming a protrusion. Dyed residual fluid had been drawn up the slope but had mostly been distributed in the region below 18 cm.

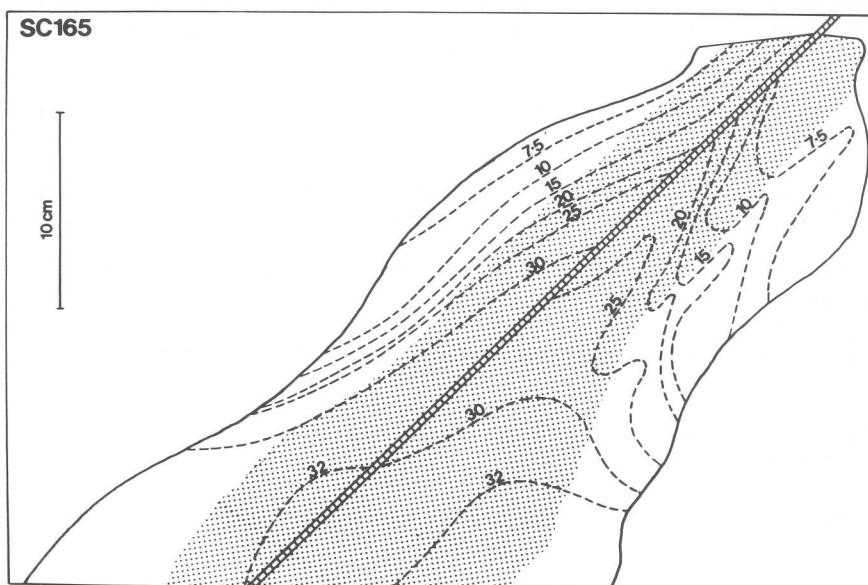


Figure 16. Contours of constant composition in experiment (10). The stippled areas represent the solid that had formed after 72 hours, just before replenishment.

The effects of replenishment on the compositional variations in the solid are shown in Figure 16. On the overhanging roof side, a clear reversal to more  $\text{Na}_2\text{CO}_3$  rich compositions is apparent at the position of the crystallization front soon after replenishment. The  $\text{Na}_2\text{CO}_3$  content again decreases beyond this position. On the inclined floor side no reversal is evident. Above about 15 cm the compositional gradient in the fluid was essentially unchanged by the replenishment process (Figure 14) and no compositional reversal could be expected in the solid

product. Below 15 cm, where the replenishment brought increasingly  $\text{Na}_2\text{CO}_3$ -rich solution in contact with the crystallizing front, the compositional contours in the solid curve distinctly outwards (Figure 16). This outward curvature is much more prevalent than in the equivalent experiment without replenishment (Figure 12). Subtle textural layering was visible in the solid at this position approximately parallel to the slope. A slight disconformity in the layering occurred within the solid between 8 to 18 cm height where melting back had been most evident.

## 6. CONCLUSIONS AND GEOLOGICAL IMPLICATIONS

The main conclusions from the experiments described here and from previous work on the crystallization of aqueous solutions can be summarised as follows:

- i) Crystallization along inclined surfaces can cause compositional zonation of the liquid.
- ii) Crystallization of compositionally zoned liquid along inclined surfaces can produce compositional gradients in the solid product.
- iii) Compositional contours in the solid product are generally discordant to the crystallization front.
- iv) Basal replenishment by hot, dense liquid elevates the residual zoned liquid.
- v) Remelting along the crystallization front may result from replenishment.
- vi) Compositional reversals in the solid product may develop as a result of replenishment.
- vii) In the terminology of layered intrusions, the compositional contours in the solid product can be equated with cryptic layering. Features resembling modal layering were only observed in one experiment (4) involving a multicomponent initial composition. These layers were parallel to the crystallization front.

Recent investigations of layered intrusions have uncovered marked discordances between modal layering and cryptic and phase layering (Wilson and Larsen, 1985; Klemm et al., 1986). Observations of some layered intrusions have also led Irvine (1981) and Irvine et al. (1983) to envisage that layers can form by downdip accretion from a compositionally stratified magma body. If discordance proves to be a widespread phenomenon then these relationships are likely to place important constraints on the origin of different kinds of layering.

Figure 17 illustrates the models that have been put forward to account for discordances by Irvine et al. (1983) and Wilson and Larsen (1985). Both models require the magma to be compositionally zoned, with magma compositions varying along a sloping boundary so that different minerals and solid solution compositions crystallize at different heights along the inclined floor.

The model presented by Irvine (1981) to explain features of the Muskox intrusion and by Irvine et al. (1983) related to the Stillwater Complex (Fig. 17a-c) attempted to account for large scale layering features. Cumulate layers are envisaged as crystallizing simultaneously from distinct magma layers along an inclined floor. Residual, buoyant melt is transferred upwards along the crystallization front, as described in this paper. The magma layers gradually move downwards as more buoyant melt is transferred and solid layers, growing in pursuit of their parental liquids, consequently dip inwards. Hence the process is referred to as "down-dip accretion" (Irvine et al., 1983).

In the Muskox intrusion the large scale layers make up macrocyclic units which show, for example, sequences of the type: ol+chr; ol+cpx; ol+cp+pl. The macrocyclic units vary from about 3 to 350 m thick (Irvine 1980). Small scale modal layering is rarely observed and cryptic variations were not considered in the model. Two important features should be developed if this model is to be accepted. Firstly, small scale modal layering, which develops parallel to the crystallization front, should be discordant to the cumulate layers. For the Muskox intrusion, the rarity of small scale modal layering makes this point difficult to establish. Secondly, individual cumulate layers should wedge out down-dip when cyclic units are repeated by magma replenishment. According to the available borehole data, Muskox cumulate layers do not appear to wedge out, although they do thin down-dip (Irvine, pers. comm., 1986). However, with very small angles between the magma layers and the crystallization front (Fig. 17c) both these critical features would be difficult to identify, and an angle of less than 3° has been inferred for the Muskox intrusion (Irvine et al. 1983). However, large-scale layers at the Honningsvaag Intrusive Suite, north Norway, wedge out towards the centre of the intrusion when cyclic units are repeated (Robins et al., this volume).

Wilson and Larsen (1985) observed discordant relations between small scale modal layering and cryptic and phase layering in the Hyllingen Series of the Fongen-Hyllingen intrusion. Large scale rhythmic or cyclic units are not developed. The fact that modal layering is concordant with a major compositional regression reflecting gradual magma replenishment strongly implies that it develops parallel to the advancing crystallization front. The angle of discordance between the magma layers and the crystallization front for the Hyllingen Series is inferred to have been up to about 20°. Cryptic variations are envisaged as reflecting compositional variations in the zoned magma, so that cryptic layering dips at an angle less than the crystallization front (Fig. 17D). A gradual compositional regression, developed over a stratigraphic thickness of about 500 m, is explained by crystallization during elevation of the zoned magma in response to the continual, slow influx of dense magma (Fig. 17E, F).

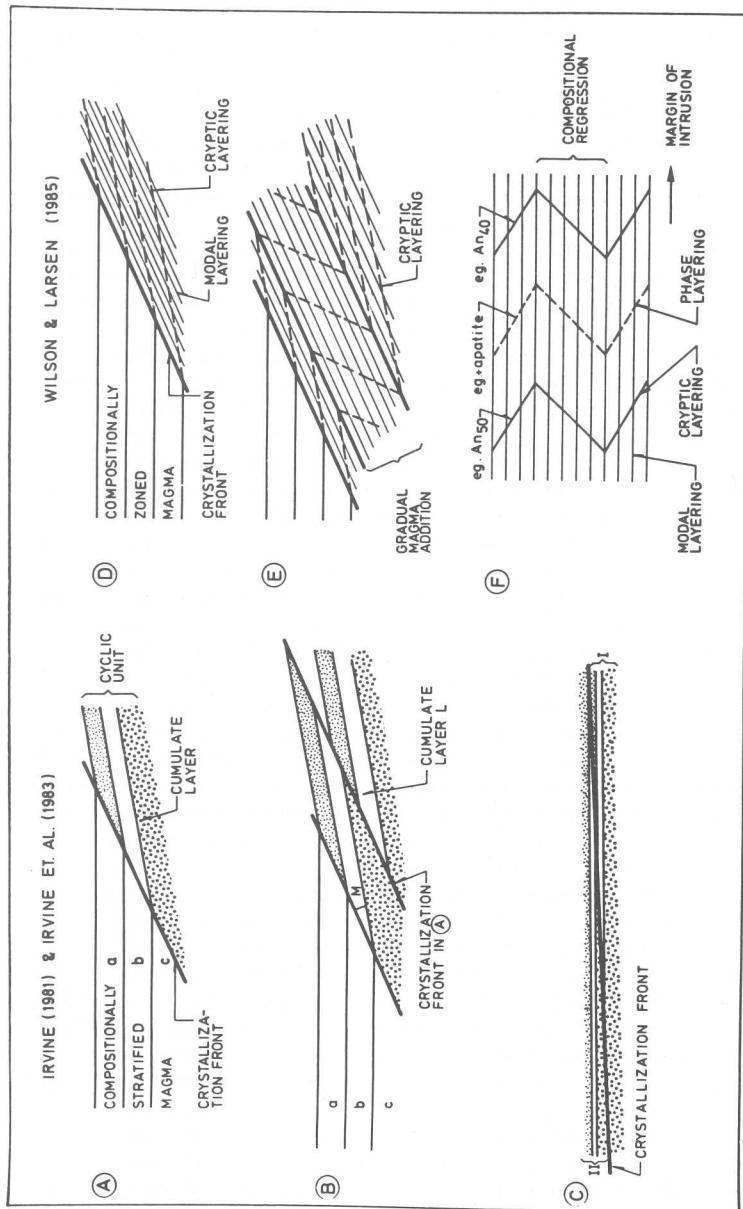


Fig. 17. Models of crystallization of zoned magma along an inclined floor. A-C "Downdip accretion" (Irvine, 1981; Irvine et al., 1983). D-E Model of Wilson and Larsen (1985). A. Cumulate layers growing from zoned magma along a downdip accretion front. B. Influx of dense magma elevates the stratified magma and the cumulate layers are repeated, which causes cumulate layers (e.g. L) to wedge out down-dip. C. Repetition of cyclic units (I and II) by magma influx illustrated with a slightly inclined crystallization front (ca. 3°). D. Cryptic layering reflects the magma zonation while modal layering develops parallel to the inclined crystallization front. E. Crystallization during slow elevation of the zoned magma produces a gradual compositional reversal. F. Cryptic and phase layering will be discordant to modal layering and will have a "Z" pattern.

The difference between the two models is thus largely in the features they attempt to explain:

	Irvine (1981) & Irvine et al (1983)	Wilson & Larsen (1985) & Wilson et al. (this vol)
Layering features	Large scale layers; cyclic units	Small scale modal layering; cryptic and phase layering
Inclination of crystallization front	<3°	<20°
Magma replenishment	Rapid	Slow

In the early stages of the experiments involving rapid cooling, a quench effect was initially produced in which compositions became more "primitive" away from the cooling front. This process could potentially produce a compositional reversal at the base of a layered intrusion, as discussed below. It is, however, the later stages of the rapidly cooled experiments and the slowly cooled ones which are most relevant for comparison with the crystallization models. The experiments demonstrate that if a compositional gradient exists in the liquid there will be the predicted discordance between the trace of the crystallization front and compositional contours in the solid, confirming one important aspect of the models in Fig. 17.

In the experiments individual double-diffusive layers are usually in the order of a few cm thick. They usually merge with adjacent layers as the experiments progress, and they may wedge out laterally. Double-diffusive layers may give rise to cusps on the crystallization front, but the cusps migrate down (or up) with their parental double-diffusive layer. No evidence of the previous existence of individual double-diffusive layers or of cusps has been observed in the interior of the solid blocks. However, in layered intrusions it is conceivable that small scale modal layering could show undulations which reflect the former presence of a cusped crystallization front. The inclination of the crystallization front and the size of the cusps would be critical if such features are to be identified on outcrop scale.

Whether magma layers (e.g. b in Fig. 17A) are individual double-diffusive convective layers, as envisaged by Irvine (1981) and Irvine et al. (1983), or are subdivided into a series of smaller ones, is an open question. Where compositionally distinct, internally homogeneous, cumulate layers are produced (Fig. 17A), it seems likely that individual parental magma layers convect as single units. Where continuous cryptic layering is produced, without sharp steps, the parental magma seems unlikely to have had abrupt compositional breaks; the zoned magma may be subdivided into many double-diffusive layers with small compositional steps between them. In view of the important role of double-diffusive convection in these models, their likely scale and duration in magmas requires investigation.

The experiments suggest a possible mechanism for producing reversals in mineral compositions close to the contacts of layered intrusions. It is quite common to find reverse cryptic layering with ferromagnesian minerals becoming increasingly Mg-rich away from the margin (Wilson and Engell-Sorensen, 1986). In the experiments the amount of trapped melt in the solid is recorded by  $\text{Na}_2\text{CO}_3$  content and gives a measure of the efficiency with which residual liquid is convected away from the crystallization front. In the initial stages rapid cooling freezes eutectic melt trapped between the  $\text{Na}_2\text{SO}_3 \cdot 10\text{H}_2\text{O}$  dendrites, but as cooling rate decreases the residual liquid can escape more effectively so that the  $\text{Na}_2\text{CO}_3$  content increases inwards even though the adjacent liquid must be decreasing in  $\text{Na}_2\text{CO}_3$  content. This initial outward increase in  $\text{Na}_2\text{CO}_3$  could be analogous to the inward decrease in Fe/Mg ratio of minerals in intrusions, representing the effects of rapid cooling in the early stages of crystallization. Initially much liquid could be trapped, producing a rock with high Fe/Mg ratios due to equilibration with abundant intercumulus melt. As cooling and crystallization with abundant intercumulus melt. As cooling and crystallization proceed less melt is trapped and the Fe/Mg ratio decreases. This is essentially the process envisaged by Raedeke and McCallum (1984) to explain the compositional reversal at the base of the Stillwater Complex. There are, however, other processes which could cause reversals near contacts (Wilson et al., this vol.)

Firm evidence in layered intrusions of remelting associated with magma replenishment is, by its nature, difficult to establish. It is, however, most likely to occur as a result of rapid replenishment and abrupt compositional reversals associated with replenishment events may in part be a result of remelting.

Discordant layering relations may develop by processes other than by direct magmatic crystallization from compositionally zoned magma bodies. There is increasing evidence that compaction of partially molten cumulate rocks and intercumulus convection can cause changes of mineral compositions due to migration of intercumulus melt (Irvine, 1980; McKenzie, 1984; Sparks et al., 1986; Kerr and Tait, 1986; McKenzie, 1987). These processes can, for example, cause Fe/Mg ratios in ferromagnesian minerals to change, and could thus cause discordances between modal and cryptic layering. In addition to downdip accretion compaction is an attractive mechanism to cause layering to dip into the centre of intrusions.

#### ACKNOWLEDGEMENTS

RSJS and HEH are supported by the BP Venture Research Unit and the NERC. RJW was supported by a Carlsberg Fellowship during sabbatical leave at Cambridge. We thank Neil Irvine for a helpful review of the paper. Sandra Last typed the manuscript.



## REFERENCES

- Chen CF, Turner JS (1980) Crystallization in a double-diffusive system. *J Geophys Res* 85: 2573-2593.
- Hebditch DJ (1975) Contribution concerning the solidification problem. In "Moving Boundary Problems in Heat Flow and Diffusion" Ockendon JR and Hodgkins WR (editors) Oxford Clarendon Press.
- Huppert HE, Turner JS (1980) Ice blocks melting into a salinity gradient. *J Fluid Mech* 100: 367-384.
- Huppert HE, Worster NG (1985) Dynamic solidification of a binary melt. *Nature* 314: 703-707.
- Huppert HE, Sparks RSJ, Wilson RJ, Hallworth MA (1986) Cooling and crystallization at an inclined plane. *Earth Planet Sci Letts* 79: 319-328.
- Irvine TN (1980) Magmatic infiltration metasomatism, double-diffusive fractional crystallization, and adcumulus growth in the Muskox and other layered intrusions. In "Physics of Magmatic Processes" Hargreaves RB (editor): 325-374.
- Irvine TN (1981) A liquid-density controlled model for chromitite formation in the Muskox intrusion. *Carnegie Institute of Washington Year Book* 80: 317-323.
- Irvine TN, Keith DW, Todd SG (1983) The J-M Platinum-palladium reef of the Stillwater Complex, Montana: II. Origin by double-diffusive convective magma mixing and implications for the Bushveld Complex. *Econ Geol* 78: 1287-1334.
- Kerr RC, Tait SR (1986) Crystallization and compositional convection in porous media with application to layered igneous intrusions. *J Geophys Res* 91: 3591-3608.
- Klemm DD, Ketterer S, Riechhardt F, Steindl J, Weber-Diefenbach K (1985) Implication of vertical and lateral compositional variations across the pyroxene marker and its associated rocks in the upper part of the Main Zone in the Eastern Bushveld Complex. *Econ Geol* 80: 1007-1015.
- Leitch AM (1985) Laboratory models of magma chambers. PhD Thesis Australian National University.
- McBirney AR (1980) Mixing and unmixing of magmas. *J Volcanol Geothermal Res* 7: 357-371.
- McBirney AR, Baker BH, Nilson RH (1985) Liquid fractionation. Part I: Basic principles and experimental simulations. *J Volcanol Geothermal Res* 24: 1-24.
- McKenzie DP (1984) The generation and compaction of partially molten rock. *J Petrol* 25: 713-765.
- McKenzie DP (1987) Compaction in sedimentary and igneous rocks. *Jour Geol Soc Lond* (in press)
- Raedeke LD, McCallum IS (1984) Investigations in the Stillwater Complex: Part II. Petrology and petrogenesis of the Ultramafic Series. *J Petrol* 23: 395-420.
- Robins B, Haukvik L, Jansen S (this volume) The organization and internal structure of cyclic units in the Honningsvaag Intrusive Suite, North Norway: implications for intrusive mechanisms, double-diffusive convection and pore-magma migration.

- Sparks RSJ, Huppert HE, Kerr RC, McKenzie DP, Tait SR (1985) Postcumulus processes in layered intrusions. *Geol Mag* 122: 555-568.
- Turner JS, Gustafson LB (1981) Fluid motions and compositional gradients produced by crystallization or melting at vertical boundaries. *J Volcanol Geotherm Res* 11: 93-125.
- Wilson JR, Engell-Sorensen O (1986) Basal reversals in layered intrusions: evidence of emplacement of compositionally stratified magma. *Nature* (in press).
- Wilson JR, Larsen SB (1985) Two dimensional study of a layered intrusion: the Hyllingen Series, Norway. *Geol Mag* 122: 97-124.
- Wilson JR, Menuge J, Pedersen S, Engell-Sorensen O (this volume). The southern part of the Fongen-Hyllingen layered mafic complex, Norway: emplacement and crystallization of compositionally stratified magma.